ORIGINAL PAPER

# Astragaloside IV — mediated endothelial progenitor cell exosomes promote autophagy and inhibit apoptosis in hyperglycemic damaged endothelial cells *via* miR-21/PTEN axis

Wu Xiong[1], Xin-ling Huang[1], Cheng-yu Li[2], Xiao-liang Wang[3], Hong-wei Lan[1], Ting-ting Wang[1], Zi-lin Chen[2], Qian-pei Yang[2], Ai-lin Hu[2], Yi-fei Xia[2], Fu-rong Zhu[1], Zhong-zhi Zhou[1]

[1]Department of Burns and Plastic Surgery, the First Affiliated Hospital of Hunan University of Chinese Medicine, Hunan, China

[2]College of Integrated Traditional Chinese and Western Medicine, Hunan University of Chinese Medicine, Hunan, China

[3]Department of Anesthesia and Operation, the First Affiliated Hospital of Hunan University of Chinese Medicine, Hunan, China

**Abstract**

**Introduction.** As one of the basic components of Astragalus, Astragaloside IV (AS-IV) has a protective effect on endothelial injury caused by diabetes. AS-IV stimulated endothelial progenitor cells (EPCs) to secrete exosomes loaded with miR-21. This study aimed to investigate the effects of AS-IV-mediated EPCs exosomal miR-21 (EPC-exos-miR-21) on high glucose (HG) damaged endothelial cells.

**Materials and methods.** After the isolation of EPCs derived from fetal umbilical cord blood, exosomes of EPCs were obtained by differential centrifugation. The morphology of exosomes was observed by electron microscopy. The particle size distribution of exosomes was detected by Nanoparticle Tracking Analysis. Human umbilical vein endothelial cells (HUVECs) were treated with 33 mM glucose to establish an HG injury model. Flow cytometry and TUNEL assay were used to characterize the surface markers of primary EPCs and the apoptosis of HUVECs. The gene and protein expression were detected by qPCR, immunofluorescence, and Western blotting. A dual luciferase assay was used to verify the targeting relationship of miR-21 with PTEN.

**Results.** HG environment led to time- and dose-dependent inhibition and enhancement of autophagy and apoptosis in HUVECs. AS-IV stimulated EPCs to secrete exosomes loaded with miR-21. Exosomes secreted by EPCs pretreated with AS-IV [EPC-exo(ASIV)] promoted autophagy and inhibited apoptosis in HG-impaired HUVECs. PTEN is a target of miR-21. MiR-21 carried by EPC-exo(ASIV) repressed PTEN expression in HG-impaired HUVECs. In contrast, p-AKT, p-mTOR, p-PI3K, cleaved PARP and PARP levels were upregulated. Compared to the HG group, the expression of autophagy regulatory genes (ATG5, beclin1 and LC3) was enhanced in the EPC-exo(ASIV) group and EPC-exo(ASIV)-miR-21 mimic group. In contrast, apoptosis-positive regulatory genes (Bax, caspase-3 and caspase-9) were attenuated. Further overexpression of PTEN reversed the expression of these genes.

**Conclusions.** AS-IV-mediated EPC-exos-miR-21 could enhance autophagy and depress apoptosis in HG-damaged endothelial cells *via* the miR-21/PTEN axis. *(Folia Histochemica et Cytobiologica 2022, Vol. 60, No. 4, 323–334)*

**Correspondence address:**
Zhong-zhi Zhou
No.95, middle Shaoshan Road, Yuhua District,
Changsha City, Hunan Province, China
e-mail: 3z_cl@163.com

## Introduction

Diabetes mellitus (DM) is a serious threat to human health, with an increasing incidence annually. The damage to the cells caused by a chronic high glucose (HG) environment triggers abnormalities in the structure and function of the related organs [1]. Chronic hyperglycemia is an independent risk factor for endothelial cell dysfunction [2]. DM induces a diminution in the number and function of different pro-angiogenic cell types, the first to suffer are endothelial progenitor cells (EPCs) [3, 4]. It has been shown that EPCs play a crucial role in maintaining endothelial cell homeostasis and normal function [5]. However, the specific mechanisms by which EPCs ameliorate endothelial cell dysfunction are unclear.

EPCs isolated from human umbilical cord blood improve endothelial cell function and contribute to vascular repair in balloon-injured rats through the paracrine action of exosomes (EPC-exos) [6]. Recent studies have shown that EPC-exos contain a large number of miRNAs, molecules and proteins, which are involved in the regulation of endothelial cell function [7]. For example, EPC-exos loaded with miR-210 act as a repair agent for hypoxia/reoxygenation (H/R) damaged endothelial cells by improving mitochondrial function [8]. Therefore, EPCs may act on endothelial cells *via* paracrine exosomes as an important pathway.

Astragaloside IV (AS-IV) is the most prominent active component of Radix astragali [9]. AS-IV has been widely recognized in preventing HG-induced endothelial dysfunction [10, 11]. In preliminary experiments, we found that EPCs incubated with AS-IV secreted exosomes [EPC-exo(ASIV)] loaded with miR-21. EPC-exo(ASIV) co-cultured with human umbilical vein endothelial cell (HUVECs) significantly enhanced the proliferation of HG-impaired endothelial cells.

Compared to healthy individuals, people with diabetes have a lower plasma miR-21 level [12]. The aberrant expression of miR-21 may contribute to the development of diabetes-related diseases [13]. In the diseases such as glioma, atherosclerosis, and diabetic nephropathy, researchers have identified the targeted regulation of PTEN by miR-21 [14–16]. PTEN signaling pathway has an essential role in regulating cellular autophagy [17]. Impaired autophagy of endothelial cells leads to endothelial dysfunction in diabetes, and the HG environment inhibits endothelial cell autophagy, which in turn triggers endothelial cell apoptosis [18]. Therefore, the repair of impaired autophagy in endothelial cells under HG stress may have a beneficial effect on the treatment of diabetes mellitus.

Thus, we hypothesized that AS-IV promotes the secretion of exosomes loaded with miR-21 from EPCs, which act on HG-damaged endothelial cells *via* the PTEN signaling pathway. This process may involve the regulation of autophagy and apoptosis in endothelial cells.

## Materials and methods

**Cell culture and treatment.** Human Umbilical Vein Endothelial Cells (HUVECs, HG-NC080, Abiowell, China) were cultured in endothelial cell growth medium-2 (EGM-2, BulletKit, Lonza, CC-3156 and CC-4176). HUVECs were pretreated with phenol red-free low glucose Dulbecco's Modified Eagle Medium (D-MEM, D5796, Sigma) supplemented with 1% fetal bovine serum (FBS) for 12 h and then placed in EGM-2 [19].

According to different experimental purposes, the cells were randomly grouped and correspondingly treated as follows: Control group (5.5 mM glucose-treated HUVECs), HG group (33 mM glucose-treated HUVECs), HG+ EPC-exo(A-SIV) group (33 mM glucose-treated HUVECs with 100 $\mu$M ASIV-induced exosomes secreted by EPCs co-culture), HG+ EPC-exo(ASIV)-NC mimic group (exosomes secreted by EPCs transfected with NC mimic plasmids after 100 $\mu$M ASIV intervention were co-cultured with 33 mM glucose-treated HUVECs), HG+ EPC-exo(ASIV)-miR-21 mimic group (exosomes secreted by EPCs transfected with miR-21 mimic plasmids after 100 $\mu$M ASIV intervention were co-cultured with 33 mM glucose-treated HUVECs). HG+ EPC-exo(ASIV)-miR-21 mimic+oe-PTEN group (exosomes secreted by EPCs transfected with miR-21 mimic after 100 $\mu$M ASIV intervention were co-cultured with HUVECs treated with 33 mM glucose and transfected with oe-PTEN plasmid).

**Isolation and identification of EPCs and their exosomes.** The isolation of human EPCs was referred to in a previous report [20]. Briefly, the cord blood was collected from the umbilical cord of healthy newborns, anticoagulated with heparin (20 U/ /mL), and then individual nucleated cells were isolated from cord blood. The cells were resuspended in the EGM-2 medium. Cells were cultured in an incubator at 37°C, with 5% $CO_2$ and saturated humidity to reach 80% confluency, and then the cells were trypsinized for passaging. Identification of cells was performed when the cells presented a shuttle shape. Flow cytometry was used to detect surface markers CD31, CD34, CD45 and CD133 of EPCs.

Exosomes were isolated by differential centrifugation as previously described [21]. Exosome morphology was observed by transmission electron microscopy (TEM). Exosome diameter was analyzed by Nanoparticle Tracking Analysis (NTA) technique. Exosome surface markers CD63, CD9 and CD81, were detected by Western blot.

**Immunofluorescence.** After treatment, the HUVECs were fixed with 4% paraformaldehyde for 30 min, then blocked with 5% bovine serum albumin (BSA) at 37°C for 60 min. Slides were added dropwise with the appropriate dilution of Anti-LC3 antibody (18725-1-AP, 1:50, Proteintech, Rosemont, IL, USA) overnight at 4°C. Then slides were dropwise added with 50~100 $\mu$L of CoraLite488-conjugated Goat Anti-Rabbit IgG(H+L) (SA00013-2, 1:200, Proteintech) and incubated for 90 min at 37°C. DAPI (Wellbio, Hunan, China) working solution was used to stain nuclei for 10 min at 37°C. After blocking with buffered glycerol, the cell slides were placed under a fluorescent microscope for observation.

**Flow cytometry.** Approximately $1 \times 10^6$ EPCs were placed in a 1.5 mL centrifuge tube each and resuspended with 200 $\mu$L of phosphate-buffered saline (PBS). The EPCs were incubated with 5 $\mu$L of antibody for 30 min, avoiding light. The cells were then washed with 1 mL of PBS and repeated twice. 200 $\mu$L of PBS was used to resuspend the cells again. The cell suspensions were filtered through nylon mesh and detected by flow cytometry (A00-1-1102, Beckman, Brea, CA, USA). The antibodies used for the flow cytometry assay were purchased from ebioscience: CD31 (item number: 17-0319-42, 0.5 $\mu$g), CD34 (item number: 17-0349-42, 0.25 $\mu$g), CD45 (item number: 17-0459-42, 0.06 $\mu$g) and CD133 (item number: 17-1338-42, 0.125 $\mu$g).

HUVECs from different treatment groups were digested with EDTA-free trypsin and centrifuged at 2000 rpm for 5 min. Approximately $2 \times 10^5$ cells were collected and suspended with 500 $\mu$L of Binding buffer. Then, HUVECs were incubated with 5 $\mu$L Annexin V-APC and 5 $\mu$L Propidium Iodide (KGA1030, KeyGEN BioTECH, Nanjing, China) at room temperature and away from light for 10 min, respectively. Within 1 h, the apoptosis level was determined by flow cytometry.

**Real-time quantitative polymerase chain reaction (qPCR).** Total RNA was extracted from HUVECs with Trizol (ThermoScientific, USA). RNA was reverse transcribed to cDNA by mRNA Reverse Transcription Kit (CW2569, Cwbio, Beijing, China) or miRNA Reverse Transcription Kit (CW2141, Cwbio, Beijing, China). The expression levels of genes were analyzed by SYBR Green. U6 and GAPDH were used as internal controls, and the $2^{-\Delta\Delta CT}$ method was used to assess the expression of hsa-miR-21-5p and mRNA. All primers in this study were synthesized by Shanghai Biotech, China (Table 1).

**Western blot.** Cells or exosomes were lysed by RIPA lysis solution (AWB0136, Abiowell, Hunan Province, China) and centrifuged at 4°C for 15 min at 12000 rpm. Protein concentration was determined according to the BCA Protein Quantification Kit (AWB0104a, Abiowell) instructions. After protein separation with 10% isolation gel, it was transferred to the NC membrane. The membranes were sealed with 5% skim milk powder. The membrane was incubated with a primary antibody overnight at 4°C. After sufficient washing, diluted HRP goat anti-mouse IGG (SA00001-1, 1:5000, Proteintech) or HRP goat anti-rabbit IGG (SA00001-2, 1:6000, Proteintech) was incubated with the membranes at room temperature for 90 min.

The membranes were incubated with enhanced chemiluminescent (ECL, Abiowell) for 1 min and imaged using a gel imaging system (Chemiscope 6100, Shanghai, China). The primary antibodies used for the Western blot assay were: LC3 (18725-1-AP, 1:500, Proteintech), AKT (10176-2-AP, 1:1000, Proteintech), mTOR (ab32028, 1:2000, abcam, UK ), PI3K (20584-1-AP, 1:200, Proteintech), PTEN (22034-1-AP, 1:5000, Proteintech), P-AKT (28731-1-AP, 1:3000, Proteintech), PARP (#9542, 1:1000, CST, USA), Cleaved PARP (#5625, 1:1000, CST), P-mTOR (ab109268, 1:3000, Abcam), P-PI3K (ab278545, 0.5 $\mu$g/mL, Abcam), CD63 (25682-1-AP, 1:300, Proteintech), CD9 (60232-1-Ig, 1:5000, Proteintech), CD81 (66866-1-Ig, 1:3000, Proteintech), ATG5 (ab109490, 1:5000, abcam), beclin1 (11306-1-AP, 1:1000, Proteintech), Bcl-2 (ab59348, 1:500, abcam), P62 (18420-1-AP, 1:4000, Proteintech), Bax (50599-2-Ig, 1:5000, Proteintech), Caspase-3 (19677-1-Ap, 1:1000, Proteintech), Caspase-9 (10380-1-AP, 1:300, Proteintech) and $\beta$-actin (66009-1-Ig, 1:5000, Proteintech).

**Dual luciferase assay.** Phg-mirtarget-PTEN WT-3U was co-transfected with hsa-miR-21 mimics/miRNA NC in target cells 293A (Abiowell). After 24 h of transfection, the lysed cells were added to Luciferase Assay Reagent II following the protocol provided by Dual-Luciferase® Reporter Assay System (Item No. E1910, Promega, Madison, WI, USA), and a chemiluminescence detector (Glomax 20/20. Promega) to quantify firefly luciferase activity. Stop & Glo® reagent was then added to quantify the fluorogenic luciferase activity.

**TUNEL assay.** HUVECs apoptosis was detected by referring to the manufacturer's instructions of the Tunel Apoptosis Detection Kit (40306ES50, Yeasen, Shanghai, China). Representative images were acquired by fluorescence microscopy. TUNEL-positive signal is green fluorescence, and the nuclear staining signal is blue.

**Statistical analysis.** Experimental data were subjected to Student's $t$-test or one-way ANOVA using Graphpad Prism 8.0 software (Graphpad Software, Inc., CA, USA). Data were presented as mean ± standard deviation. All experiments were repeated at least 3 times. P-values less than 0.05 were considered statistically significant.

## Results

### *HG treatment inhibited autophagy and promoted apoptosis in HUVECs*

To understand the effect of HG on endothelial cell autophagy, we first treated HUVECs with different glucose concentrations. We examined the expression of LC3 II/I in the HUVECs cultured with HG after 24 h, 48 h, and 72 h, respectively. As shown in Fig. 1, the level of LC3 II/I in HUVECs was suppressed correspondingly with increased glucose concentration. With the same concentration of glucose treatment, the level of LC3 II/I in HUVECs was gradually depressed as the treatment time increased. Further, immu-
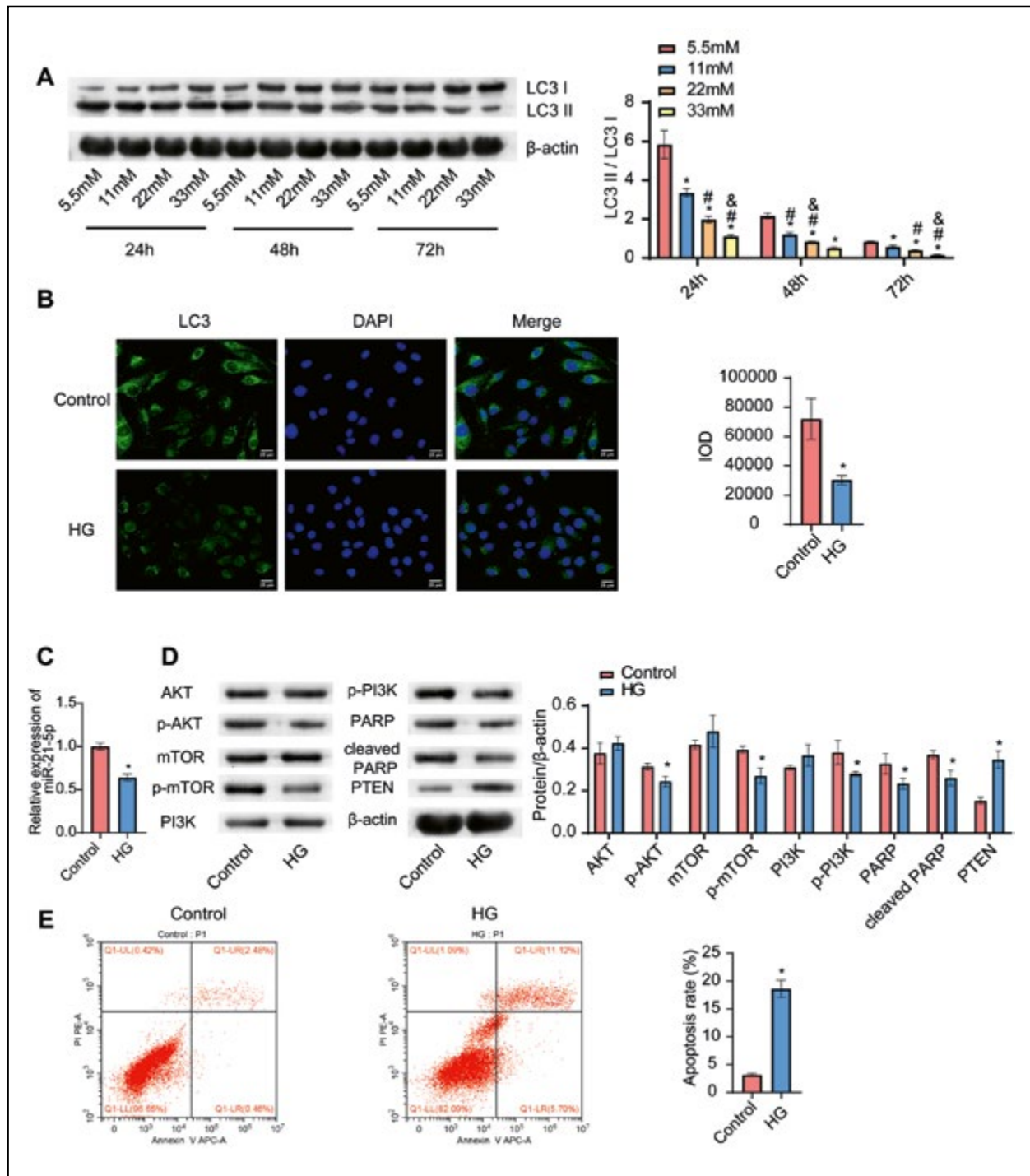
**Figure 1.** High glucose (HG, 33mM) treatment inhibited autophagy and promoted apoptosis in HUVECs. **A.** Expression of LC3 II/I in HUVECs was detected by Western bloting after treatment with different glucose concentrations for 24 h, 48 h, and 72 h, respectively. **B.** Immunofluorescence analysis of LC3 expression (green fluorescence) in HUVECs. **C.** Quatitative PCR was used to detect the expression of miR-21 in HUVECs. **D.** Western bloting was used to examine the expression of AKT, p-AKT, mTOR, p-mTOR, PI3K, p-PI3K, PARP, cleaved PARP and PTEN. **E.** Flow cytometry was used to detect the apoptosis rate of HUVECs. $^{*}P < 0.05$ *vs.* 5.5 mM glucose or control group, $^{#}P < 0.05$ *vs.* 11 mM glucose group, $^{&}P < 0.05$ *vs.* 22 mM glucose group.

nofluorescence assay results showed that LC3 was significantly inhibited after HG treatment of HUVECs for 72 h (Fig. 1B). HG treatment caused a decrease in miR-21 expression in HUVECs (Fig. 1C). According to Fig. 1D, HG treatment resulted in a markedly impaired phosphorylation of AKT, mTOR and PI3K. Both PARP and cleaved PARP were downregulated by HG stimulation. In contrast, HG treatment induced high PTEN protein expression in HUVECs. We also discovered that HG treatment increased apoptosis in HUVECs (Fig. 1E).

### AS-IV promoted the secretion of exosomes loaded with miR-21 from EPCs

We obtained EPCs by identifying surface markers CD31, CD34, CD45, and CD133 by flow cytometry. EPCs were positive for CD31, CD34, CD133, and negative for CD45 (Fig. 2A). The EPC exosome morphology was presented in Fig. 2B, whose diameter ranged from 100–200 nm (Fig. 2C). CD63, CD9, and CD81 were positively expressed in the exosomes (Fig. 2D). Next, we treated EPCs with different concentrations of AS-IV and found that AS-IV dramatically promoted the expression of miR-21 in EPC exosomes (Fig. 2E). AS-IV at a concentration of $100\,\mu$M exhibited the most pronounced promotion of miR-21 expression in EPC exosomes. Therefore, we selected this concentration for the subsequent investigations.

### AS-IV-mediated EPC exosomes facilitated autophagy and suppressed apoptosis in HG-damaged HUVECs

We first treated EPCs with $100\,\mu$M AS-IV and transfected them with miR-21 mimic to make miR-21 stably overexpressed in EPC exosomes (Fig. 3A). We noticed that HG stimulation decreased LC3II/I, ATG5, beclin1 and Bcl-2 expression in HUVECs, while P62, Bax, caspase-3 and caspase-9 expression were increased. The expression of these proteins was reversed in the HG+EPC-exo(ASIV) and HG+EPC-exo(ASIV)-miR-21-mimics groups compared to the HG group. The effect of EPC-exo(ASIV) transfected with miR-21-mimics on up-, or down-regulation of these proteins was apparently stronger than treatment without miR-21 mimic transfection (Fig. 3B). HG stimulation led to a significant increase in the apoptosis rate of HUVECs compared to the control group. EPC-exo(ASIV) with or without miR-21-mimics markedly rescued the surge in apoptosis rate of HUVECs caused by HG stimulation. EPC-exo(ASIV) transfected with miR-21 mimic had a superior inhibitory effect on apoptosis than single EPC-exo(ASIV) treatment (Fig. 3C).

### PTEN is a target of miR-21

We verified a targeting interaction between miR-21 and PTEN by a dual luciferase reporter (Fig. 4A). Further, we transfected miR-21 mimics into HUVECs, and the expression of miR-21 was upregulated in HUVECs (Fig. 4B). We found that PTEN expression in HUVECs transfected with miR-21 mimic was significantly reduced at both mRNA and protein levels relative to the control group (Fig. 4C, D).

### AS-IV mediated EPC exosomes improved HG-impaired HUVECs function via miR-21/ /PTEN axis

To verify whether AS-IV-mediated EPC exosomes improve HG-damaged endothelial cells *via* the miR-21/PTEN axis, we transfected HUVECs with oe-PTEN plasmids. We observed that PTEN overexpression did not affect the expression of miR-21 in HUVECs (Fig. 5A). In addition, compared to the HG group, EPC-exo(ASIV) and EPC-exo(ASIV)-miR-21 mimic treatment decreased PTEN expression in HG-impaired HUVECs (Fig. 5A). Compared with the HG group, ATG5, beclin1, LC3 and Bcl-2 expression was increased, and P62, Bax, caspase-3 and caspase-9 expression was decreased in HG+EPC-exo(ASIV) group, and miR-21 mimic amplified the up- and down-regulation of HG+EPC-exo(ASIV). In comparison with HG+EPC-exo(ASIV)- miR-21-mimics+oe-NC group, ATG5, beclin1, LC3 and Bcl-2 expression were down-regulated in HG+EPC-exo(ASIV)- miR--21-mimics+oe-PTEN group, and P62, Bax, caspase-3 and caspase-9 expression was elevated (Fig. 5B). We further verified the expression of these genes at the protein level, and Western blot results showed that the expression of these proteins was consistent with the mRNA level (Fig. 5C).

Next, we examined the activation of AKT, mTOR and PI3K downstream of PTEN, as well as PARP cleavage. The expression of p-AKT, p-mTOR, p-PI3K, PARP, and cleaved PARP was reduced in the HG group compared to the control group. EPC-exo(ASIV) reversed the expression of these proteins in the presence of HG damage. Transfection of miR-21-mimics magnified the reversal of EPC-exo(ASIV). The expression of p-AKT, p-mTOR, p-PI3K and cleaved PARP was decreased in the HG+EPC-exo(A-SIV)- miR-21-mimics+oe-PTEN group as compared to the HG+EPC-exo(ASIV)- miR-21-mimics group (Fig. 5D). An increase in TUNEL-positive cells in the HG group compared to the control group. The rate of TUNEL-positive cells was reduced in the HG+EPC--exo(ASIV) group compared to the HG group, and further reduced after transfection with miR-21 mimic. The rate of TUNEL-positive cells was increased in the
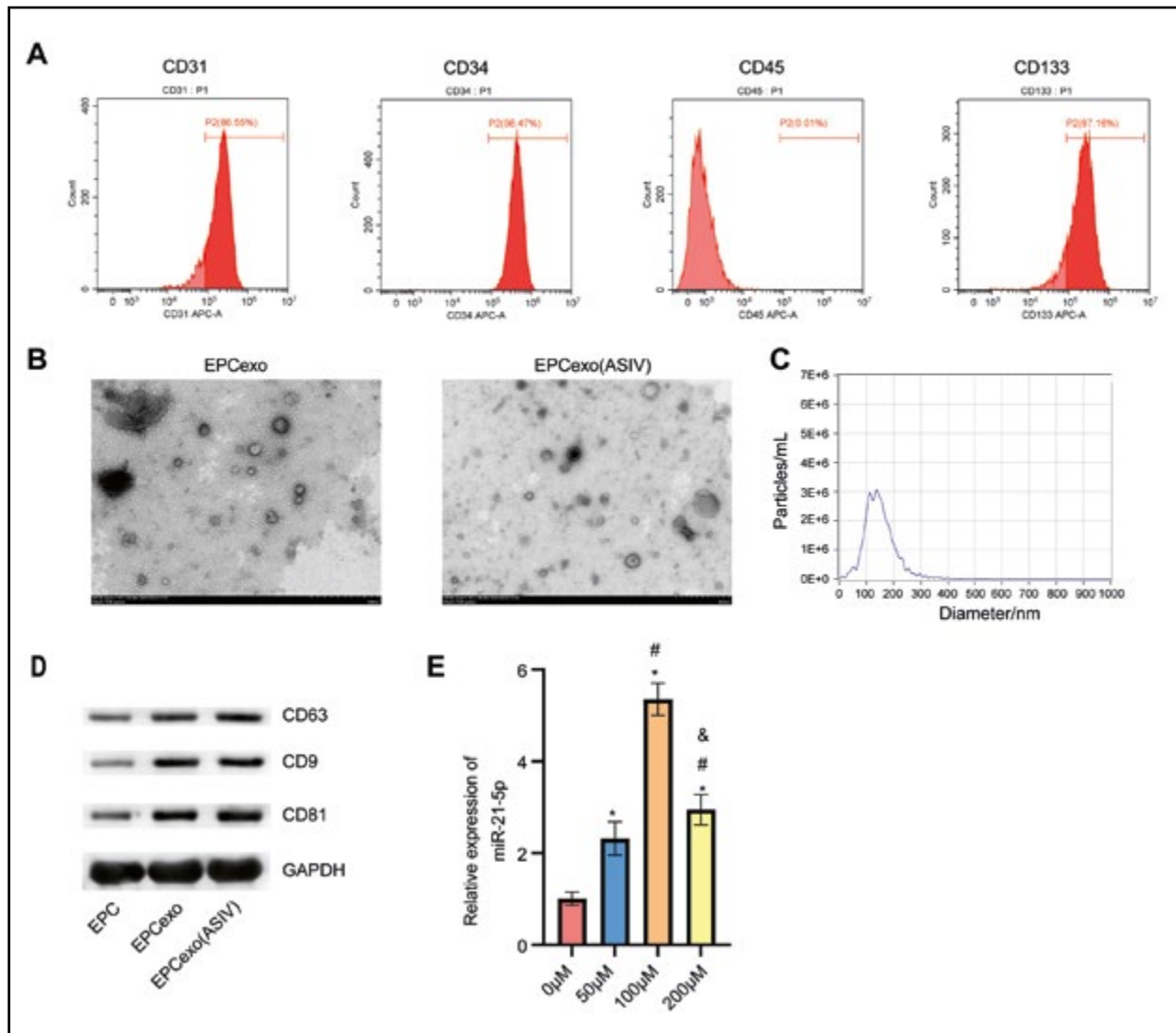
**Figure 2.** Astragaloside IV (AS-IV) promoted the secretion of exosomes loaded with miR-21 from endothelial progenitor cells (EPCs). **A.** The surface markers (CD31, CD34, CD45, and CD133) of EPCs were assessed by flow cytometry. **B.** Electron micrographs of EPC exosomes. **C.** The exosome diameter was analyzed by NTA. **D.** Western bloting was used to identify surface markers CD63, CD9 and CD81 on exosomes. **E.** EPC exosomes were collected 24 h after incubation of EPCs with 0 $\mu$M, 50 $\mu$M, 100 $\mu$M and 200 $\mu$M AS-IV and the expression of miR-21 in exosomes was detected by qPCR. $^*$P < 0.05 $vs.$ 0 $\mu$M AS-IV group, $^\#$P < 0.05 $vs.$ 50 $\mu$M gAS-IV group, $^\&$P < 0.05 $vs.$ 100 $\mu$M AS-IV group.

HG+EPC-exo(ASIV)- miR-21-mimics group compared with the HG+EPC-exo(ASIV)- miR-21-mimics+o-e-PTEN group (Fig. 5E).

## Discussion

Autophagy dysregulation is closely associated with DM. Studies have pointed out autophagy deficiency may cause endoplasmic reticulum or mitochondrial dysfunction that triggers DM [22]. Muralidharan *et al.* [23] found that the autophagy of pancreatic β-cells is impaired in type 1 DM. Our findings showed that

HG environment leads to a time- and dose-dependent inhibition of autophagy in HUVECs. On the other hand, HG stimulation exacerbated HUVECs apoptosis, which may be related to blocked autophagy. AS-IV protects cardiomyocytes from HG-induced injury through the miR-34a-mediated autophagic pathway [24]. Also, AS-IV enhances autophagy through the SIRT-NF-κB p65 axis to inhibit the HG-induced epithelial-mesenchymal transition of podocytes [25]. In the ischemia/reperfusion (I/R) model, AS-IV exerts neuroprotective effects by promoting P62-LC3 autophagy to downregulate apoptosis [26]. These studies
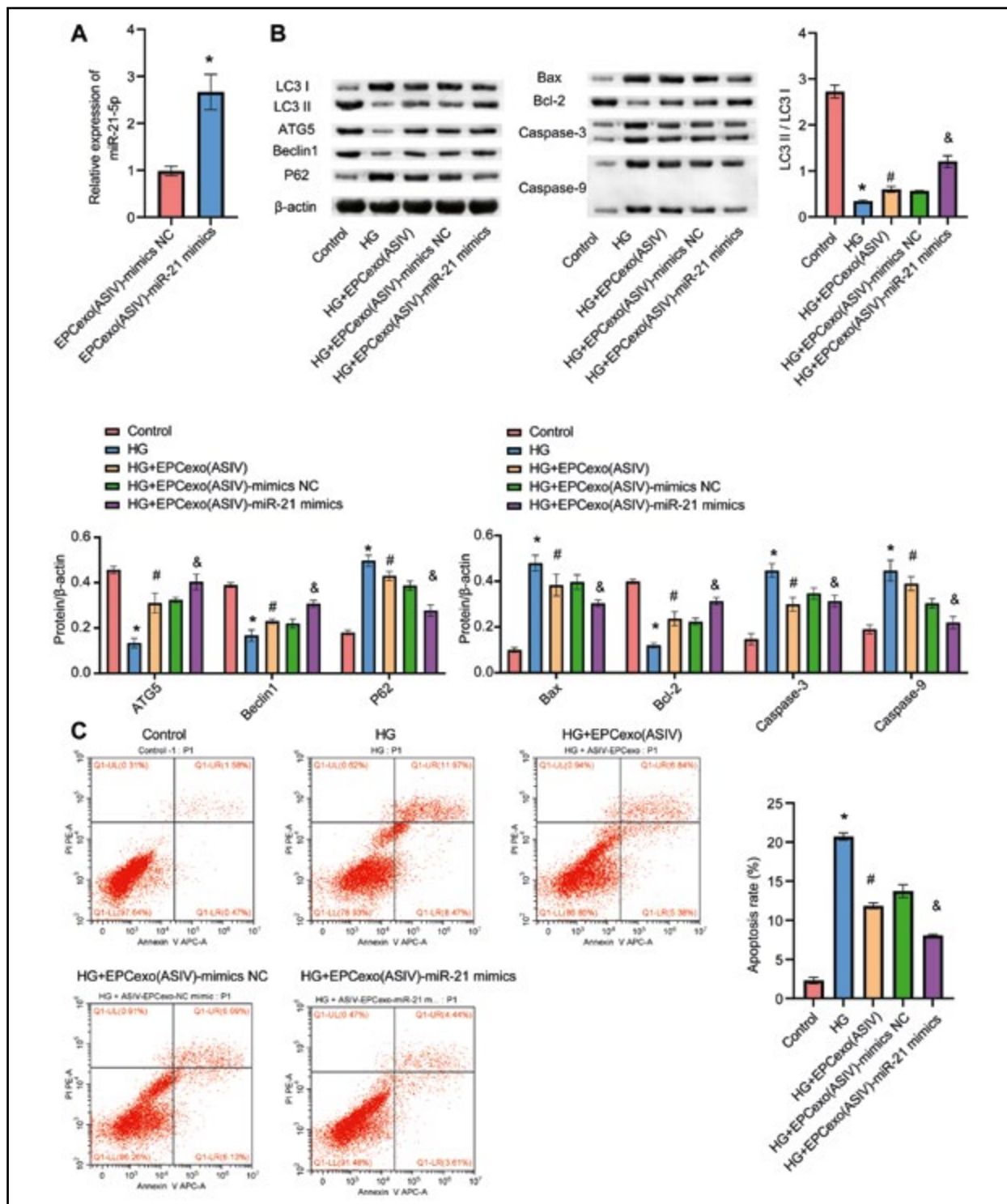
**Figure 3.** AS-IV-mediated EPC exosomes facilitated autophagy and suppressed apoptosis in HG-damaged HUVECs. **A.** Expression of miR-21 in exosomes was detected by qPCR. **B.** Western blot was used to detect the expression of autophagy-associated proteins (ATG5, beclin1, LC3II/I, and P62) and apoptosis-associated proteins (Bax, Bcl-2, Caspase-3, and Caspase-9) in control and miR-21 transfected HUVECs cultured in HG medium. **C.** Flow cytometry was performed to assess the apoptotic rate of HUVECs. *P < 0.05 *vs.* EPCexo(ASIV)-mimics NC or control group. #P < 0.05 *vs.* HG group, &P < 0.05 *vs.* HG+EPCexo(ASIV)-mimics NC group.
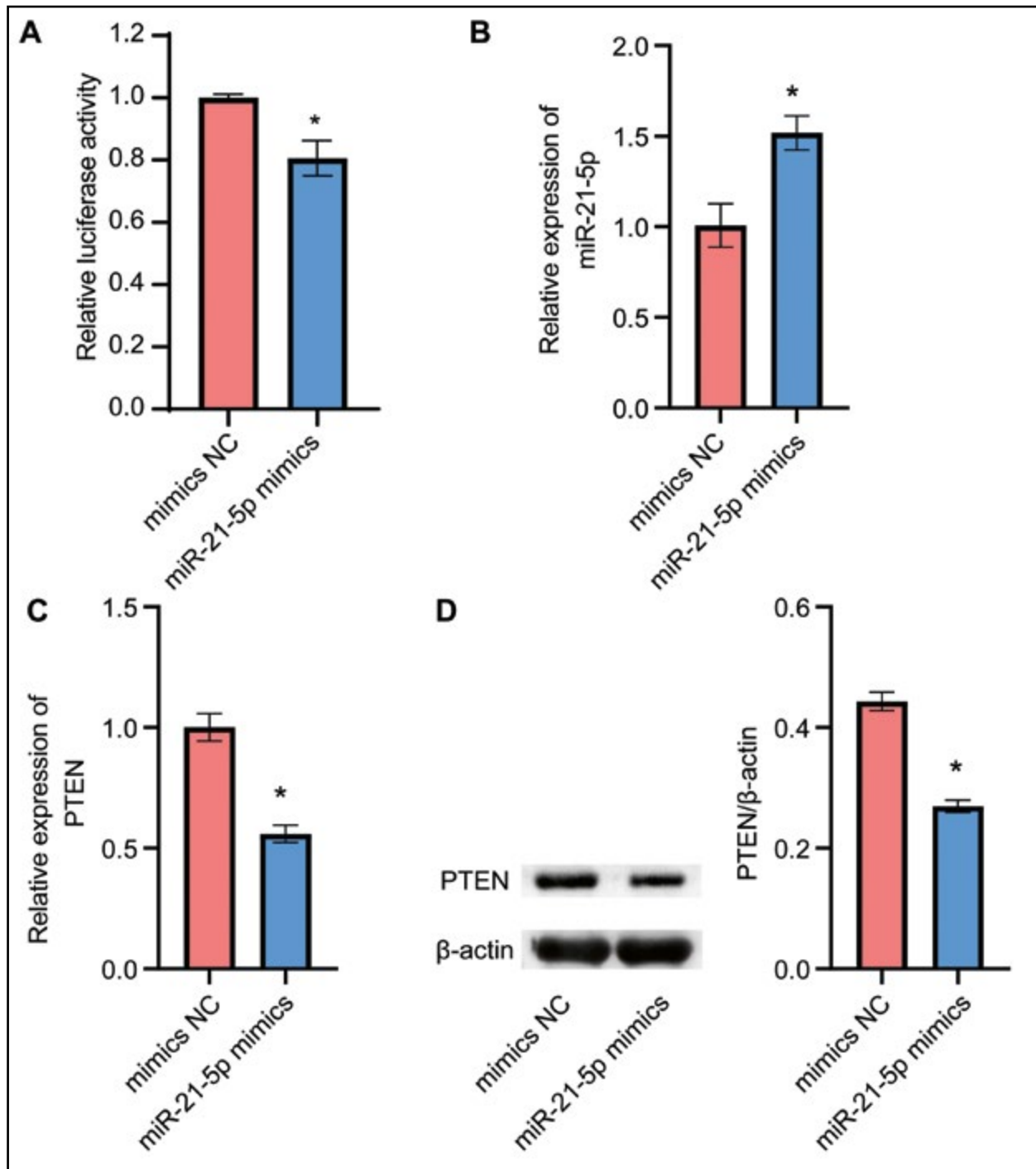
**Figure 4.** PTEN is a target of miR-21. **A.** miR-21 targeted PTEN was verified by Dual luciferase reporter after transfection of miR-21 mimic by HUVECs. **B, C.** The expression of miR-21 and PTEN at mRNA level was detected by qPCR. **D.** The protein level of PTEN was assessed by Western bloting. *$P < 0.05$ *vs.* mimics NC group.

suggested that AS-IV has a promising potential to improve cellular autophagy.

AS-IV has been demonstrated to attenuate the development of DM through multiple mechanisms. For example, AS-IV can reduce blood glucose in DM mice by inhibiting hepatic glycogen phosphorylase and glucose-6-phosphatase activities [27]. AS-IV

prevents the progression of diabetic nephropathy by suppressing eNOS acetylation and enhancing eNOS 1177-site phosphorylation [28]. By inhibiting oxidative stress and calpain-1 activation, AS-IV prevents HG-induced vascular endothelial dysfunction [29]. Additionally, it has been revealed that AS-IV exhibits a marked improvement in oxidized LDL-induced EPC
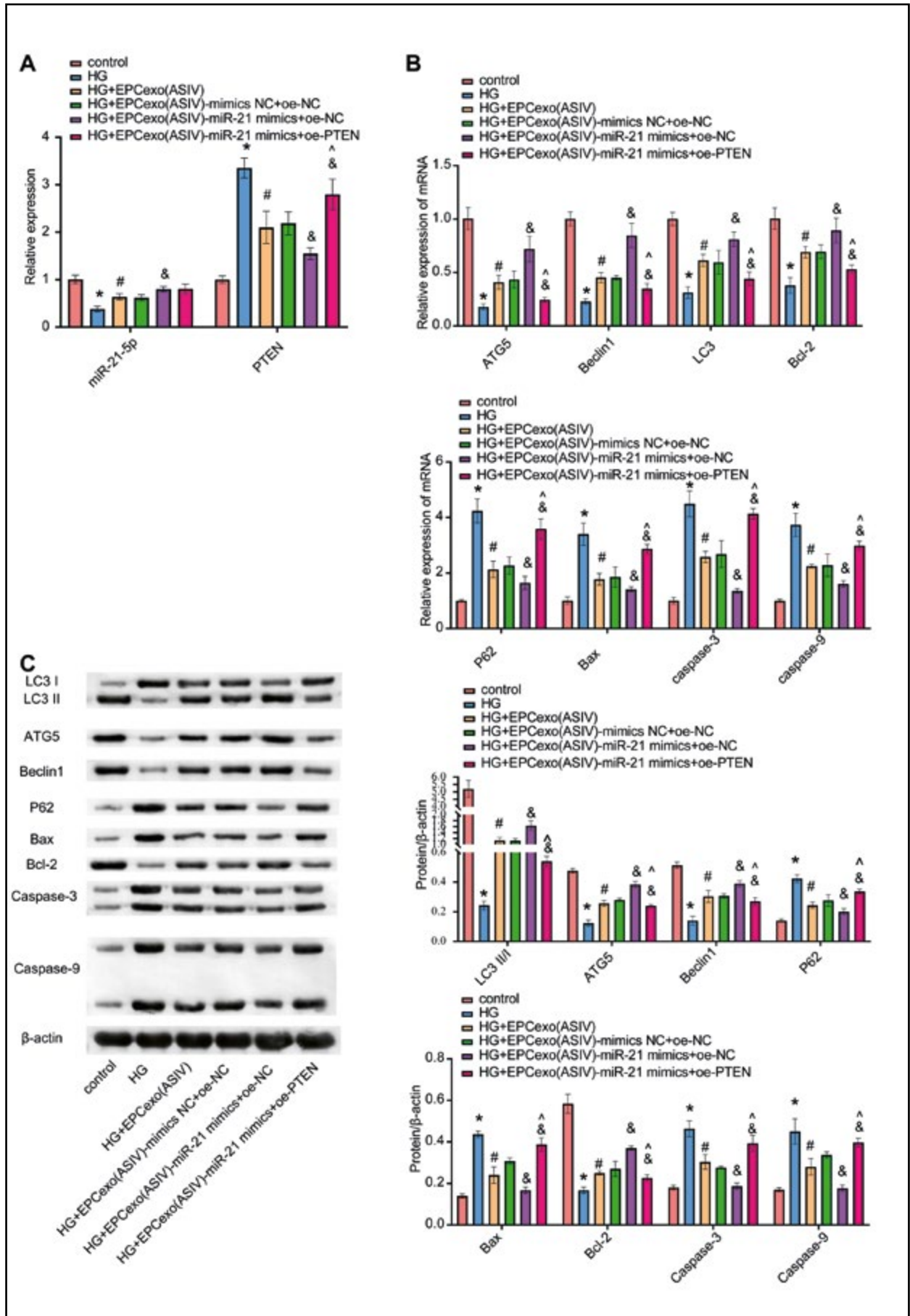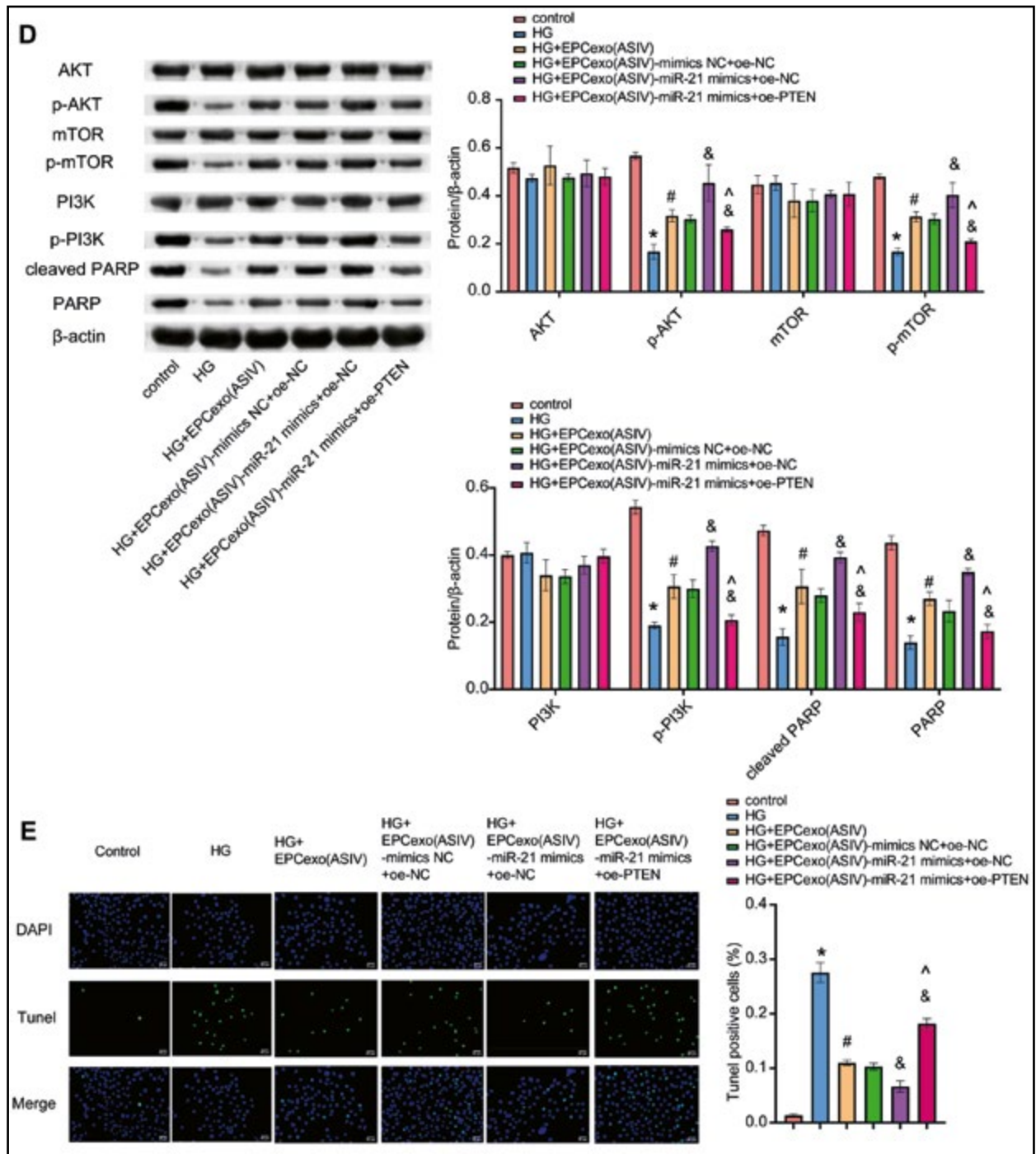
**Figure 5.** AS-IV-mediated EPC exosomes improved HG-impaired HUVECs function *via* miR-21/PTEN axis. **A.** QPCR was performed to detect the expression of miR-21 and PTEN in HUVECs. **B, C.** The expression of autophagy-associated genes (ATG5, Beclin1, LC3, and P62) and apoptosis-associated genes (Bax, Bcl-2, Caspase-3, and Caspase-9) was confirmed by qPCR and Western blots in HUVECs. **D.** Western bloting was used to test the expression of AKT, p-AKT, mTOR, p-mTOR, PI3K, p-PI3K, PARP and cleaved PARP proteins. **E.** The apoptosis was analyzed by TUNEL assay in HUVECs. *$P < 0.05$ *vs.* control group. #$P < 0.05$ *vs.* HG group. &$P < 0.05$ *vs.* HG+EPCexo(ASIV)-mimics NC+oe-NC group. ^$P < 0.05$ *vs.* HG+EPCexo(ASIV)-miR-21 mimics+oe-NC group.

dysfunction *via* the LOX-1/NLRP3 inflammatory vesicle pathway [30]. Our team previously found that AS-IV improves the function of exosomes secreted by human EPCs [31]. In the present study, we found that AS-IV stimulated EPCs to secrete exosomes loaded with miR-21. In the HG environment, AS-IV-mediated EPC exosomes promoted enhanced autophagy and decreased apoptosis in HUVECs. These data imply that AS-IV-EPCs might repair the dysfunction of HG-damaged endothelial cells through a paracrine

exosomal pathway. EPCs have been proven effective in assisting endothelial cell repair *via* the exosome pathway [32]. For instance, EPC-exo promotes the survival of damaged endothelial cells by mediating the transfer of angiotensin-converting enzyme 2 [33]. AS-IV mediates the paracrine secretion of exosomes from adipose stem cells to promote fibroblasts against photoaging [31]. Therefore, AS-IV-mediated EPC-derived exosomes may be a prospective new approach for the treatment of DM.

PTEN is a molecular switch molecule that regulates cellular metabolism and autophagy [34]. PRDX1 was shown to activate autophagy through the PTEN/AKT signaling pathway to prevent cisplatin-induced neuronal damage in spiral ganglia [35]. We confirmed that PTEN is a target of miR-21. Overexpression of PTEN reversed the inhibitory effect of miR-21 carried by EPC-exo(ASIV) on apoptosis and the promotion of autophagy in HG-damaged endothelial cells. Intriguingly, miR-21 carried by EPC-exo(ASIV) allowed activation of the PI3K/AKT/mTOR signaling pathway in HG-stimulated HUVECs *via* inhibiting PTEN expression. Tuning PI3K/AKT/mTOR-mediated autophagy has also been designed in therapeutic strategies for various tumors [36]. It is known that autophagy can inhibit HG-induced apoptosis in cardiac microvascular endothelial cells through the mTOR signaling pathway [37]. Besides, PARP-1 was involved in $H_2O_2$-induced autophagy *via* the AMPK/mTOR signaling pathway, which regulates the apoptosis of vascular endothelial cells [38]. Our study found that EPC-exo(ASIV) reversed HG-induced PARP and cleaved PARP inhibition. This may be a key regulator of EPC-exo(ASIV)-mediated PI3K/AKT/mTOR regulation of downstream cell autophagy and apoptosis.

In summary, AS-IV-mediated EPC secretion of miR-21-rich exosomes. Further, AS-IV-mediated EPC exosomes promoted autophagy and inhibited apoptosis in HG-damaged endothelial cells *via* the miR-21/PTEN axis.

## Author's declaration

The authors declare that this manuscript has not been submitted to other journals.

## Fundings

## References

1. Cole JB, Florez JC. Genetics of diabetes mellitus and diabetes complications. Nat Rev Nephrol. 2020; 16(7): 377–390, doi: 10.1038/s41581-020-0278-5, indexed in Pubmed: 32398868.
2. Xie X, Chen Y, Liu J, et al. High glucose induced endothelial cell reactive oxygen species via OGG1/PKC/NADPH oxidase pathway. Life Sci. 2020; 256: 117886, doi: 10.1016/j.lfs.2020.117886, indexed in Pubmed: 32497631.
3. Wils J, Favre J, Bellien J. Modulating putative endothelial progenitor cells for the treatment of endothelial dysfunction and cardiovascular complications in diabetes. Pharmacol Ther. 2017; 170: 98–115, doi: 10.1016/j.pharmthera.2016.10.014, indexed in Pubmed: 27773788.
4. Zahran AM, Mohamed IL, El Asheer OM, et al. Circulating endothelial cells, circulating endothelial progenitor cells, and circulating microparticles in type 1 diabetes mellitus. Clin Appl Thromb Hemost. 2019; 25: 1076029618825311, doi: 10.1177/1076029618825311, indexed in Pubmed: 30760002.
5. Kim KA, Shin YJ, Kim JH, et al. Dysfunction of endothelial progenitor cells under diabetic conditions and its underlying mechanisms. Arch Pharm Res. 2012; 35(2): 223–234, doi: 10.1007/s12272-012-0203-y, indexed in Pubmed: 22370777.
6. Li X, Chen C, Wei L, et al. Exosomes derived from endothelial progenitor cells attenuate vascular repair and accelerate reendothelialization by enhancing endothelial function. Cytotherapy. 2016; 18(2): 253–262, doi: 10.1016/j.jcyt.2015.11.009, indexed in Pubmed: 26794715.
7. Li X, Chen C, Wei L, et al. Exosomes derived from endothelial progenitor cells attenuate vascular repair and accelerate reendothelialization by enhancing endothelial function. Cytotherapy. 2016; 18(2): 253–262, doi: 10.1016/j.jcyt.2015.11.009, indexed in Pubmed: 26794715.
8. Ma X, Wang J, Li J, et al. Loading MiR-210 in endothelial progenitor cells derived exosomes boosts their beneficial effects on hypoxia/reoxygeneation-injured human endothelial cells via protecting mitochondrial function. Cell Physiol Biochem. 2018; 46(2): 664–675, doi: 10.1159/000488635, indexed in Pubmed: 29621777.
9. Li L, Hou X, Xu R, et al. Research review on the pharmacological effects of astragaloside IV. Fundam Clin Pharmacol. 2017; 31(1): 17–36, doi: 10.1111/fcp.12232, indexed in Pubmed: 27567103.
10. Qiao Y, Fan CL, Tang MK. Astragaloside IV protects rat retinal capillary endothelial cells against high glucose-induced oxidative injury. Drug Des Devel Ther. 2017; 11: 3567–3577, doi: 10.2147/DDDT.S152489, indexed in Pubmed: 29263652.
11. You L, Fang Z, Shen G, et al. Astragaloside IV prevents high glucoseinduced cell apoptosis and inflammatory reactions through inhibition of the JNK pathway in human umbilical vein endothelial cells. Mol Med Rep. 2019; 19(3): 1603–1612, doi: 10.3892/mmr.2019.9812, indexed in Pubmed: 30628687.
12. Giannella A, Radu CM, Franco L, et al. Circulating levels and characterization of microparticles in patients with different degrees of glucose tolerance. Cardiovasc Diabetol. 2017; 16(1): 118, doi: 10.1186/s12933-017-0600-0, indexed in Pubmed: 28927403.
13. Dai B, Li H, Fan J, et al. MiR-21 protected against diabetic cardiomyopathy induced diastolic dysfunction by targeting gelsolin. Cardiovasc Diabetol. 2018; 17(1): 123, doi: 10.1186/s12933-018-0767-z, indexed in Pubmed: 30180843.

14. Guo X, Qiu W, Liu Q, et al. Immunosuppressive effects of hypoxia-induced glioma exosomes through myeloid-derived suppressor cells via the miR-10a/Rora and miR-21/Pten Pathways. Oncogene. 2018; 37(31): 4239–4259, doi: 10.1038/s41388-018-0261-9, indexed in Pubmed: 29713056.

15. Zhu J, Liu B, Wang Z, et al. Exosomes from nicotine-stimulated macrophages accelerate atherosclerosis through miR-21-3p/PTEN-mediated VSMC migration and proliferation. Theranostics. 2019; 9(23): 6901–6919, doi: 10.7150/thno.37357, indexed in Pubmed: 31660076.

16. Guo J. Effect of miR-21 on Renal Fibrosis Induced by Nano-SiO$_2$ in Diabetic Nephropathy Rats via PTEN/AKT Pathway. J Nanosci Nanotechnol. 2021; 21(2): 1079–1084, doi: 10.1166/jnn.2021.18631, indexed in Pubmed: 33183446.

17. Wang Ye, Liu Y, Du X, et al. Berberine Reverses Doxorubicin Resistance by Inhibiting Autophagy Through the PTEN/Akt/mTOR Signaling Pathway in Breast Cancer. Onco Targets Ther. 2020; 13: 1909–1919, doi: 10.2147/ott.s241632.

18. Fetterman JL, Holbrook M, Flint N, et al. Restoration of autophagy in endothelial cells from patients with diabetes mellitus improves nitric oxide signaling. Atherosclerosis. 2016; 247: 207–217, doi: 10.1016/j.atherosclerosis.2016.01.043, indexed in Pubmed: 26926601.

19. Niu C, Chen Z, Kim KT, et al. Metformin alleviates hyperglycemia-induced endothelial impairment by downregulating autophagy via the Hedgehog pathway. Autophagy. 2019; 15(5): 843–870, doi: 10.1080/15548627.2019.1569913, indexed in Pubmed: 30653446.

20. Hu H, Wang B, Jiang C, et al. Endothelial progenitor cell-derived exosomes facilitate vascular endothelial cell repair through shuttling miR-21-5p to modulate Thrombospondin-1 expression. Clin Sci (Lond). 2019; 133(14): 1629–1644, doi: 10.1042/CS20190188, indexed in Pubmed: 31315970.

21. Lässer C, Eldh M, Lötvall J. Isolation and characterization of RNA-containing exosomes. J Vis Exp. 2012(59): e3037, doi: 10.3791/3037, indexed in Pubmed: 22257828.

22. Lim H, Lim YM, Kim KH, et al. A novel autophagy enhancer as a therapeutic agent against metabolic syndrome and diabetes. Nat Commun. 2018; 9(1): 1438, doi: 10.1038/s41467-018-03939-w, indexed in Pubmed: 29650965.

23. Muralidharan C, Conteh AM, Marasco MR, et al. Pancreatic beta cell autophagy is impaired in type 1 diabetes. Diabetologia. 2021; 64(4): 865–877, doi: 10.1007/s00125-021-05387-6, indexed in Pubmed: 33515072.

24. Zhu Y, Qian X, Li J, et al. Astragaloside-IV protects H9C2(2-1) cardiomyocytes from high glucose-induced injury via miR-34a-mediated autophagy pathway. Artif Cells Nanomed Biotechnol. 2019; 47(1): 4172–4181, doi: 10.1080/21691401.2019.1687492, indexed in Pubmed: 31713440.

25. Wang X, Gao Y, Tian N, et al. Astragaloside IV inhibits glucose-induced epithelial-mesenchymal transition of podocytes through autophagy enhancement via the SIRT-NF-κB p65 axis. Sci Rep. 2019; 9(1): 323, doi: 10.1038/s41598-018-36911-1, indexed in Pubmed: 30674969.

26. Zhang Yi, Zhang Y, Jin XF, et al. The role of astragaloside IV against cerebral ischemia/reperfusion injury: suppression of apoptosis via promotion of P62-LC3-autophagy. Molecules. 2019; 24(9): 1838, doi: 10.3390/molecules24091838, indexed in Pubmed: 31086091.

27. Lv L, Wu SY, Wang GF, et al. Effect of astragaloside IV on hepatic glucose-regulating enzymes in diabetic mice induced by a high-fat diet and streptozotocin. Phytother Res. 2010; 24(2): 219–224, doi: 10.1002/ptr.2915, indexed in Pubmed: 19610026.

28. Fan Y, Fan H, Zhu B, et al. Astragaloside IV protects against diabetic nephropathy via activating eNOS in streptozotocin diabetes-induced rats. BMC Complement Altern Med. 2019; 19(1): 355, doi: 10.1186/s12906-019-2728-9, indexed in Pubmed: 31805910.

29. Nie Qu, Zhu L, Zhang L, et al. Astragaloside IV protects against hyperglycemia-induced vascular endothelial dysfunction by inhibiting oxidative stress and Calpain-1 activation. Life Sci. 2019; 232: 116662, doi: 10.1016/j.lfs.2019.116662, indexed in Pubmed: 31323271.

30. Qian W, Cai X, Qian Q, et al. Astragaloside IV protects endothelial progenitor cells from the damage of ox-LDL via the LOX-1/NLRP3 inflammasome pathway. Drug Des Devel Ther. 2019; 13: 2579–2589, doi: 10.2147/dddt.s207774, indexed in Pubmed: 31440038.

31. Xiong W, Xiao H, Lan HW, et al. Effects of Astragaloside IV on exosome secretion and its microRNA-126 expression in human endothelial progenitor cells. Zhonghua Shao Shang Za Zhi. 2020; 36(12): 1183–1190, doi: 10.3760/cma.j.cn501120-20191222-00466 , indexed in Pubmed: 33379855.

32. Zhang J, Chen C, Hu B, et al. Exosomes derived from human endothelial progenitor cells accelerate cutaneous wound healing by promoting angiogenesis through erk1/2 signaling. Int J Biol Sci. 2016; 12(12): 1472–1487, doi: 10.7150/ijbs.15514, indexed in Pubmed: 27994512.

33. Wang J, Chen S, Bihl Ji. Exosome-mediated transfer of ACE2 (angiotensin-converting enzyme 2) from endothelial progenitor cells promotes survival and function of endothelial cell. Oxid Med Cell Longev. 2020; 2020: 4213541, doi: 10.1155/2020/4213541, indexed in Pubmed: 32051731.

34. Aquila S, Santoro M, Caputo A, et al. The tumor suppressor as molecular switch node regulating cell metabolism and autophagy: implications in immune system and tumor microenvironment. Cells. 2020; 9(7): 1725, doi: 10.3390/cells9071725, indexed in Pubmed: 32708484.

35. Liu W, Xu L, Wang X, et al. PRDX1 activates autophagy via the PTEN-AKT signaling pathway to protect against cisplatin-induced spiral ganglion neuron damage. Autophagy. 2021; 17(12): 4159–4181, doi: 10.1080/15548627.2021.1905466, indexed in Pubmed: 33749526.

36. Xu Z, Han Xu, Ou D, et al. Targeting PI3K/AKT/mTOR-mediated autophagy for tumor therapy. Appl Microbiol Biotechnol. 2020; 104(2): 575–587, doi: 10.1007/s00253-019-10257-8, indexed in Pubmed: 31832711.

37. Zhang Z, Zhang S, Wang Y, et al. Autophagy inhibits high glucose induced cardiac microvascular endothelial cells apoptosis by mTOR signal pathway. Apoptosis. 2017; 22(12): 1510–1523, doi: 10.1007/s10495-017-1398-7, indexed in Pubmed: 28825154.

38. Meng YY, Wu CW, Li H, et al. PARP-1 involvement in autophagy and their roles in apoptosis of vascular smooth muscle cells under oxidative stress. Folia Biol (Praha). 2018; 64(3): 103–111, indexed in Pubmed: 30394268.